Article:

Review

U-Values for Building Envelopes of Different Materials: A Review

Jiaqi Yu [1], Yu Dong [2,3], Tsung-Hsien Wang [1], Wen-Shao Chang [4,*] and Jihyun Park [5,*]

1   School of Architecture, University of Sheffield, Sheffield S10 2TN, UK; jyu89@sheffield.ac.uk (J.Y.); tsung-hsien.wang@sheffield.ac.uk (T.-H.W.)
2   School of Architecture and Design, Harbin Institute of Technology, Harbin 150001, China; dongyu.sa@hit.edu.cn
3   Key Laboratory of Cold Region Urban and Rural Human Settlement Environment Science and Technology, Ministry of Industry and Information Technology, Harbin 150001, China
4   Lincoln School of Architecture and the Built Environment, University of Lincoln, Lincoln LN6 7TS, UK
5   Department of Architecture, Ewha Womans University, Seoul 03760, Republic of Korea
*   Correspondence: wchang@lincoln.ac.uk (W.-S.C.); jh.park@ewha.ac.kr (J.P.)

Abstract: In recent decades, the issue of building energy usage has become increasingly significant, and U-values for building envelopes have been key parameters in predicting building energy consumption. This study comprehensively reviews the U-values (thermal transmittances) of building envelopes made from conventional and bio-based materials. First, it introduces existing studies related to the theoretical and measured U-values for four types of building envelopes: concrete, brick, timber, and straw bale envelopes. Compared with concrete and brick envelopes, timber and straw bale envelopes have lower U-values. The differences between the measured and theoretical U-values of timber and straw bale envelopes are minor. The theoretical U-values of concrete and brick envelopes ranged from 0.12 to 2.09 W/m²K, and the measured U-values of concrete and brick envelopes ranged from 0.14 to 5.45 W/m²K. The theoretical U-values of timber and straw bale envelopes ranged from 0.092 to 1.10 W/m²K, and the measured U-values of timber and straw bale envelopes ranged from 0.04 to 1.30 W/m²K. Second, this paper analyses the environmental factors influencing U-values, including temperature, relative humidity, and solar radiation. Third, the relationship between U-values and building energy consumption is also analysed. Finally, the theoretical and measured U-values of different envelopes are compared. Three research findings in U-values for building envelopes are summarised: (1) the relationship between environmental factors and U-values needs to be studied in detail; (2) the gaps between theoretical and measured U-values are significant, especially for concrete and brick envelopes; (3) the accuracy of both theoretical and the measured U-values needs to be verified.

Keywords: U-values; concrete envelopes; brick envelopes; timber envelopes; straw bale envelopes; building energy

1. Introduction

Building energy use continues to increase significantly around the world. The building sector accounts for around 30% of final energy use [1,2]. This exacerbates fossil fuel consumption, making it imperative to decrease energy use in the building sector [3]. In addition, this sector is also regarded as one of the most cost-efficient fields in which to reduce energy use [4]. Thus, many researchers have focused on building energy consumption in recent years [5–7].

In existing studies, building energy simulation has proven to be an important method for predicting building energy consumption [8–10]. To obtain building energy prediction results, accurate envelope parameters need to be entered into the simulation software. The thermal transmittances (U-values) of building envelopes are crucial thermal parameters [11,12].

The U-value is the rate of heat transfer across a building envelope. As shown in Equation (1), Φ is the heat transfer, A is the area in square meters, and ΔT is the temperature difference between the interior and exterior sides of the building envelope.

$$U = \Phi/(A \times \Delta T) \; [W/(m^2 \cdot K)] \tag{1}$$

The U-value shows the thermal insulation property of the building envelope. It is important for predicting building energy consumption and understanding the impacts of buildings on the environment. There are two types of U-values in existing studies: theoretical U-values obtained by formulas and measured U-values obtained by experiments.

1.1. Theoretical U-Values of Building Envelopes

The theoretical U-values of envelopes are calculated according to the ISO 6946 method [13]. Under this method, the U-value of a building envelope can be estimated by related envelope parameters, as shown in Equations (2) and (3):

$$U = 1/(R_{se} + R_{si} + R_{sum})[W/(m^2 \cdot K)] \tag{2}$$

$$R = D/\lambda[(m^2 \cdot K)/W] \tag{3}$$

where R_{se} and R_{si} are thermal resistances of the external and internal surfaces of the building envelope, correspondingly. R_{sum} is the sum of the thermal resistances of all layers within the building envelope. R is the thermal resistance of each layer, D is the thickness of each layer, and λ is the thermal conductivity of each layer in the building envelope.

Theoretical U-values may be reasonable for the initial phase of design. However, detailed parameters about some existing buildings are not available or are not maintained. The U-values of many existing building envelopes are difficult to calculate using the theoretical method.

1.2. Measured U-Values of Building Envelopes

In order to obtain U-values of envelopes in actual conditions, both laboratory and in situ measurements can be reasonable approaches. The common U-value measurement methods are shown in Figure 1. For laboratory measurement, the Hot Box Test (HBT) is a common method. Both ASTM C1363 and ISO 8990 standards are used to regulate measurement equipment and procedures [14,15]. Guarded hot box (GHB) and calibrated hot box (CHB) are two common types in HBT, as shown in Figure 1a,b. Both methods require steady-state conditions and are suitable for full-scale building components. A U-value measurement system includes (1) several heat flow sensors; (2) several temperature sensors; and (3) a data logger. The measured U-value can be calculated by Equation (4).

$$U = \frac{\sum_{j=1}^{n} q_j}{\sum_{j=1}^{n} (T_{ij} - T_{ej})} [W/(m^2 \cdot K)] \tag{4}$$

where U is the U-value of the tested envelope during the measurement period, q_j is the heat flow density at time j, and T_{ij} and T_{ej} are the temperature in the indoor and outdoor environment at time j, respectively. n is the number of recorded samples during the measurement period.

Many researchers have used these methods to measure the U-values of different types of envelopes [16–18]. For example, Yang et al. used the GHB method to investigate the U-values for straw bales with different structural details. The results showed that straw bales with plastering had lower U-values [16]. Chen et al. applied a CHB to study the U-values of double-glazing units. Comparing the measurement results with simulation results revealed a difference of less than 5%, which can be considered negligible [19]. However, the temperature and relative humidity are fixed values in laboratory measurements, and laboratory conditions are different from the actual conditions of buildings.
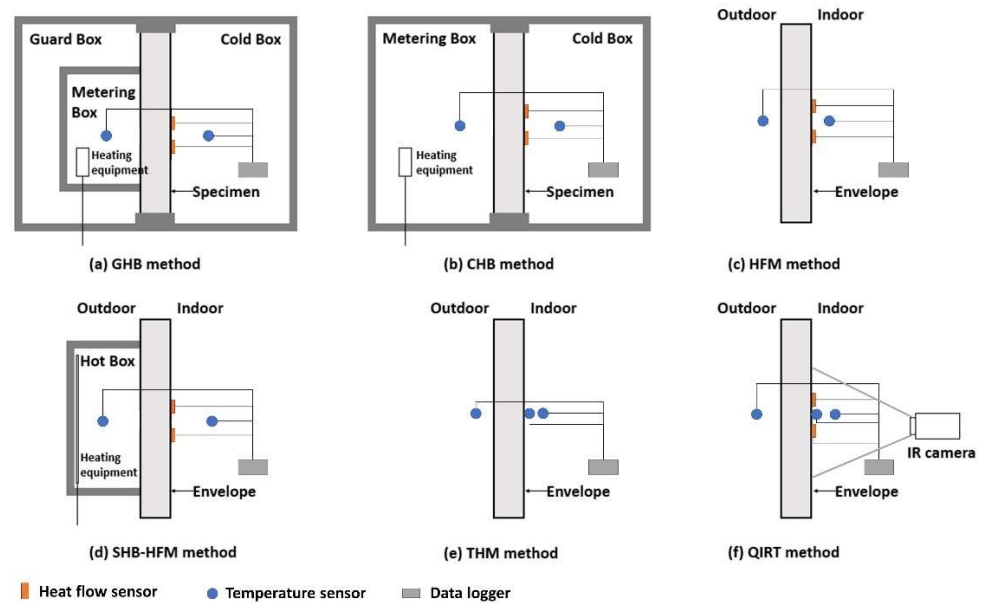
Figure 1. Schematic diagrams of laboratory and in situ U-value measurement methods.

The in situ U-value measurements have been conducted to investigate U-values in actual situations. Four methods are commonly used: the heat flow meter (HFM), the simple hot box-heat flow meter (SHB-HFM), the thermometric (THM), and the quantitative infrared thermography (QIRT). As shown in Figure 1c, the HFM method is a standardized method for in situ U-value measurement, and it is governed by ISO 9869-1 and ASTM C1155 standards [20,21]. The equipment in the HFM method includes several heat flow sensors, several temperature sensors, and a data logger. After the data have been collected, the U-value can be calculated by Equation (4). Many studies have measured the U-values of building envelopes by the HFM method on various occasions [22–24]. For example, the U-values of seven masonry envelopes were measured by this method [25], and the results showed that there was a discrepancy between the measured and theoretical U-values. The shortcoming of this method is that when the temperature difference is unstable, there may be a large error in the measured U-values.

To avoid this drawback, the SHB-HFM method was developed. In this method, a simple hot box is attached to one side of the test envelope, as shown in Figure 1d. This box has heating equipment to control the temperature difference between indoor and outdoor environments. The U-value can be calculated by Equation (4) as well. Meng et al. proposed this method and verified its feasibility through an in situ U-value measurement. The results showed that the test error of the U-value by the SHB-HFM method was only −5.97% relative to the theoretical U-value [26]. This method requires additional specialised equipment; hence, the applications of this method are limited.

The THM method is a low-cost method which needs less equipment than other methods. It requires several temperature sensors and a data logger, as shown in Figure 1e. The calculation method of measured U-values in the THM method is shown in Equations (5) and (6) [27].

$$U_j = \frac{h_i(T_{ij} - T_{sij})}{T_{ij} - T_{ej}} [W/(m^2 \cdot K)] \tag{5}$$

$$U = \frac{\sum_{j=1}^{n} U_j}{n} [W/(m^2 \cdot K)] \tag{6}$$

where U_j is the U-value of the tested envelope at time j, and T_{ij} and T_{ej} are the temperature of the indoor and outdoor environment at time j, correspondingly. T_{sij} is the internal surface temperature of the tested envelope at time j. h_i is the heat transfer coefficient of the

internal surface of the tested envelope. U is the U-value of the tested envelope during the measurement period. n is the number of recorded samples during the measurement period.

Bienvenido analysed eight tested envelopes to evaluate the advantages and shortcomings of this method. The results showed that the U-values obtained through the THM method were valid in winter, while it was difficult to obtain valid results in warmer seasons [27]. This method needs very stable indoor conditions. Thus, it is less adapted.

The QIRT method has been used widely in recent decades. This method can be conducted according to ISO 9869-2 and ASTM C1060 standards [28,29]. This method is expensive and requires specialist training. In the QIRT method, an infrared camera, temperature sensors, heat flow sensors, and a data logger are needed, as shown in Figure 1f. Compared to other methods, the QIRT method is a newer method that has been developed in recent years. There is no universal equation for calculating the U-value in this method [30]. Each new method of calculating the U-value is related to the actual conditions of in situ measurements [31]. Mahmoodzadeh et al. used the QIRT method to study the U-values of timber-framed building envelopes. They found that estimated U-values were not identical on different days due to variations in outdoor environmental parameters [32]. Climate conditions and air pollution can also influence the results obtained by the QIRT method.

In the existing literature, the theoretical U-values of building envelopes were different from the measured U-values [32–35]. The type of U-values entered into the building energy simulation affects the building energy prediction results and the energy management in the building sector. Thus, it is important to understand the differences between theoretical and measured U-values for different building envelopes. In this paper, U-values of both inorganic and bio-based envelopes (including concrete, brick, timber and straw bale envelopes) will be examined. In Section 2, theoretical and measured U-values of these four types of envelopes will be shown according to the data from existing related studies. The environmental factors affecting the U-values of building envelopes will be analysed in Section 3, while in Section 4, the studies related to energy impacts caused by U-values will be reviewed. A comparison of the theoretical and measured U-values and research gaps will be analysed in Sections 5 and 6, respectively.

2. Theoretical and Measured U-Values of Inorganic and Bio-Based Envelopes

Inorganic and bio-based envelopes are two important types of envelopes. Concrete and brick envelopes are inorganic envelopes, which are the most common worldwide [36,37]. Both timber and straw bales have been paid more attention due to the lower environmental impacts in recent years [38–41]. Using life cycle assessment (LCA), the carbon emissions of bio-based material buildings are lower than inorganic material buildings [42–44]. In this section, concrete, brick, timber, and straw bale envelopes will be the objects of the study, and existing studies will be examined to assess both the theoretical and measured U-values of these four types of envelopes.

2.1. Concrete Envelopes

As shown in Table 1, the theoretical U-values of concrete envelopes range from 0.12 to 1.61 W/m^{2}K with most concentrated around 0.15–0.50 W/m^{2}K. In U-value measurements for concrete envelopes, more research applied in situ measurements than laboratory measurements, and most used the HFM method. Reinforced concrete (RC) envelopes have been studied more than other concrete envelopes. The measured U-values of concrete envelopes range from 0.14 to 5.45 W/m^{2}K with most concentrated around 0.15–0.60 W/m^{2}K. The measured U-values in a few studies are much larger than the theoretical U-values. For example, O'Hegarty et al. found that the measured U-values of the concrete envelopes were around twice their theoretical U-values [33]. Some researchers conducted in situ measurements in winter. Because of the larger temperature difference between indoor and outdoor environments in winter, a steady heat flow can be generated in the envelopes, which can improve the accuracy of the measurement results. Several researchers mea-

sured the U-values of concrete envelopes with different orientations [23,45], and the results showed that the U-values of the north envelopes were smaller than the U-values of the envelopes with other orientations.

Table 1. Existing studies related to U-values of concrete envelopes.

Year	Envelope Type	Measurement Type	Measurement Method	Theoretical U-Value (W/m²·K)	Measured U-Value (W/m²·K)	Reference
2006	Concrete envelopes with vacuum-insulation	Laboratory measurement	GHB	NA	3.74 0.16 0.17 0.19 0.21 0.25 0.29	[46]
2014	6 types of concrete block envelopes with different structures	In situ measurement	HFM	0.23 0.25 0.27 0.30 0.32 0.33	0.22 0.34 0.34 0.37 0.56 0.39	[47]
2014	Hollow reinforced precast concrete envelopes	In situ measurement	HFM	NA	1.459 (north envelope in summer) 1.803 (east envelope in summer)	[45]
2014	A cavity envelope	In situ measurement	HFM	0.20	0.26	[48]
2015	A concrete block envelope	In situ measurement	SHB-HFM	1.315	1.22–1.26	[26]
2016	An RC envelope	In situ measurement	HFM	0.22	0.23–0.35	[49]
2017	Hollow concrete blocks	In situ measurement	HFM	NA	2.1–2.7	[50]
2017	7 types of RC envelopes	In situ measurement	HFM	0.431 0.429 0.418 0.312 0.280 0.269	0.475 (in winter) 0.479 (in winter) 0.434 (in winter) 0.316 (in winter) 0.273 (in winter) 0.269 (in winter)	[51]
2018	An RC envelope	In situ measurement	HFM	0.270	0.250–0.265	[24]
2018	A concrete block envelope	In situ measurement	HFM	0.153	0.176 (in winter)	[52]
2019	RC envelopes; lightweight concrete envelopes	In situ measurement	QIRT	0.480; 0.252	0.480 0.261	[53]
2020	RC envelopes	In situ measurement	HFM	0.333	0.400 (north envelope in summer); 0.522 (south envelope in summer); 0.393 (north envelope in winter); 0.536 (south envelope in winter)	[23]
2020	A lightweight concrete envelope	Laboratory measurement	HBT	0.313	0.314–0.323	[54]
2020	Thin precast concrete envelopes	Laboratory measurement	HBT	NA	0.144–0.555	[55]
2020	Translucent concrete envelopes	Laboratory measurement	CHB	NA	4.25 5.45	[56]

Table 1. *Cont.*

Year	Envelope Type	Measurement Type	Measurement Method	Theoretical U-Value (W/m²·K)	Measured U-Value (W/m²·K)	Reference
2021	7 types of concrete envelopes with different structures	In situ measurement	HFM	0.144 0.165 0.14 0.118 0.191 0.381 1.612	0.46 (in summer) 0.18 (in spring) 0.56 (in spring) 0.21 (in autumn) 0.64 (in winter) 1.02 (in winter) 1.46 (in winter)	[33]
2021	A lightweight concrete block envelope	In situ measurement	HFM	2.01	1.363–1.782	[35]
2021	A 3D-printed concrete envelope	In situ measurement	QIRT	NA	0.54–1.00	[57]
2022	A concrete envelope	In situ measurement	HFM	0.21	0.17–0.41	[22]
2024	A concrete envelope with internal insulation	In situ measure-ment	HFM	0.145	0.136–0.148	[58]
2024	An autoclaved concrete block envelope	Laboratory measurement	HBT	NA	0.795–1.23	[59]

2.2. Brick Envelopes

In existing studies related to the U-values of brick envelopes, the main types have included clay, limestone, hollow, perforated, red, solid, ceramic, and silica brick envelopes. As shown in Table 2, the theoretical U-values of brick envelopes range from 0.22 to 2.09 W/m²K. The thickness of the insulation is an influencing factor. For example, Albatici et al. calculated the theoretical U-value of the brick envelope as 0.225 W/m²K. The thickness of the insulation is 8 cm [60]. Marshall calculated the theoretical U-value of the brick envelope as 2.09 W/m²K. This envelope is a 222.5 mm solid brick envelope without insulation [61].

In U-value measurements for brick envelopes, more researchers applied in situ measurement methods, the most common of which was the HFM method. The measured U-values of brick envelopes range from 0.15 to 5.26 W/m²K. The majority of studies found that the theoretical U-values were close to the measured U-values with a deviation of less than 20%. However, a minority of studies found theoretical U-values to be much larger or much smaller than the measured U-values. For example, Evangelisti et al. found that the measured U-value of a tuff brick envelope was only 40% of the theoretical U-value [62]. Ratnieks et al., on the other hand, found that the measured U-value of a ceramic brick envelope was twice the theoretical U-value [52].

Table 2. Existing studies related to U-values of brick envelopes.

Year	Envelope Type	Measurement Type	Measurement Method	Theoretical U-Value (W/m²·K)	Measured U-Value (W/m²·K)	Reference
2003	A clay brick envelope	Laboratory measurement	CHB	0.302	0.304	[63]
2010	Brick envelopes	In situ measurement	QIRT	0.225	0.285	[60]
2011	2 types of limestone brick envelopes	Laboratory measurement	The Hot Disk technique	NA	3.03 5.26	[64]
2011	3 perforated brick envelopes	In situ measurement	QIRT	1.39	1.51 1.31 1.63	[65]

Year	Envelope Type	Measurement Type	Measurement Method	Theoretical U-Value (W/m²·K)	Measured U-Value (W/m²·K)	Reference
2012	A ceramic brick	In situ measurement	HFM	NA	0.97–2.56	[66]
2014	3 types of lightweight clay bricks	NA	NA	0.62 0.54 0.55	NA	[67]
2015	3 types of brick envelopes	In situ measurement	QIRT	0.30 0.57 0.44	0.37 (in winter) 0.62 (in winter) 0.51 (in winter)	[68]
2015	A fired-clay brick envelope	In situ measurement	HFM	NA	1.32	[69]
2015	2 types of hollow brick envelopes	Laboratory measurement	CHB	NA	1.24 1.20	[70]
2015	5 types of hollow bricks	Laboratory measurement	HBT	NA	0.25 0.17 0.15 0.15 0.16	[71]
2015	A solid brick envelope	In situ measurement	HFM	NA	0.428–1.933 (in summer)	[72]
2015	A tuff brick envelope; 2 types of hollow brick envelopes	In situ measurement	HFM	1.897 0.734 0.945	0.750 1.072 0.810	[62]
2016	3 types of hollow brick envelopes	In situ measurement	HFM	0.72 2.35 0.49	0.75 (in winter) 2.40 (in winter) 0.59 (in spring)	[73]
2016	3 types of solid brick envelopes	In situ measurement	HFM	0.683 0.947 0.678	0.926 0.687 0.797	[74]
2016	A brick envelope	Laboratory measurement	HBT	0.56	0.62	[17]
2017	2 types of historic red brick envelopes	In situ measurement	HFM	1.05 0.24	1.23 0.21	[75]
2017	Solid brick envelopes	In situ measurement	HFM	1.00–1.25	0.80–0.85	[76]
2018	8 types of hollow brick envelopes	In situ measurement	THM	1.18 0.57 1.50 0.56 1.10 0.76 0.45 0.48	1.03 0.59 1.39 0.45 0.98 0.38 0.48 0.88	[27]
2018	A solid brick envelope with gypsum plaster	In situ measurement	QIRT	2.09	1.57	[61]
2018	Solid brick envelopes	In situ measurement	HFM	NA	1.740 (in spring) 1.27 (in spring) 1.98 (in spring) 1.815 (in spring)	[77]
2018	2 types of ceramic brick envelopes	In situ measurement	HFM	0.151; 0.159	0.161 (in winter) 0.320 (in winter)	[52]

Table 2. *Cont.*

Year	Envelope Type	Measurement Type	Measurement Method	Theoretical U-Value (W/m²·K)	Measured U-Value (W/m²·K)	Reference
2019	2 types of hollow brick envelopes; a perforated brick envelope	In situ measurement	QIRT	0.657 0.362 0.586	0.654 0.404 0.559	[53]
2020	A silica brick envelope	In situ measurement	HFM; QIRT	0.244	0.221 (in winter) 0.229 (in winter)	[54]
2024	A pumice block envelope, two clay block envelopes	Laboratory measurement	HBT	NA	0.887–1.65 1.16–2.07 0.718–0.83	[59]

2.3. Timber Envelopes

As conventional building materials have serious impacts on the environment, bio-based building materials have been given more attention in recent decades [78–80]. Such materials can store carbon and reduce carbon emissions [42]. As an important bio-based building material, timber envelopes have gradually re-emerged because timber envelopes not only have a low environmental impact but also have a simple manufacturing process and can have high prefabrication rates [81,82].

Due to the popularity of timber envelopes, there have been a growing number of studies investigating the U-values of timber envelopes in the last decade, as shown in Table 3. In existing studies related to the U-values of timber envelopes, the main types of timber envelopes include cross-laminated timber (CLT) envelopes, oriented strand board (OSB) envelopes, light timber envelopes, plywood panel envelopes and timber frame envelopes with different insulations. The theoretical U-values of these timber envelopes range from 0.15 to 1.10 W/m²K with most concentrated around 0.15–0.20 W/m²K. Theoretical U-values were not calculated in some of these studies. This may be due to the lack of information on the thermal conductivity of some bio-based building materials, such as wood–hemp insulation panels and wheat chaff insulation panels [83,84]. Future studies on thermal conductivity will need to increase the variety of tested bio-based building materials.

In measuring the U-values of timber envelopes, in situ measurements were used more than laboratory measurements with the QIRT and HFM methods being adopted the most often. The measured U-values of these timber envelopes range from 0.04 to 0.98 W/m²K with most concentrated around 0.20–0.25 W/m²K. There are deviations between the theoretical U-values and measured U-values with the ratio of measured U-values to theoretical U-values ranging from 25% to 165%. For example, Williamson et al. investigated the thermal performance of two residential buildings using the HFM method to measure the U-values of two OSB external envelopes. The results showed that the measured U-values could be up to 1.65 times the theoretical U-values [85].

Table 3. Existing studies related to U-values of timber envelopes.

Year	Envelope Type	Measurement Type	Measurement Method	Theoretical U-Value (W/m²·K)	Measured U-Value (W/m²·K)	Reference
2010	A light timber external envelope; a CLT envelope	In situ measurement	QIRT	0.29 0.148	0.38 0.194	[60]
2014	2 types of vapour open timber frame envelopes	In situ measurement	HFM	NA	0.17–0.46 (in summer)	[86]
2014	Block and wood envelopes	In situ measurement	THM	1.1	0.67–0.98 (before retrofit) 0.26 (after retrofit)	[87]
2015	2 types of light timber envelopes	In situ measurement	QIRT	0.17 0.18	0.14 (in winter) 0.16 (in winter)	[68]

Table 3. *Cont.*

Year	Envelope Type	Measurement Type	Measurement Method	Theoretical U-Value (W/m²·K)	Measured U-Value (W/m²·K)	Reference
2015	Timber frame envelopes with wood-hemp insulation	In situ measurement	HFM	NA	0.20–0.31 (in winter)	[83]
2016	2 types of OSB envelopes	In situ measurement	HFM	0.10 0.23	0.11 (in winter) 0.38 (in winter)	[85]
2018	A timber frame envelope with wheat chaff insulation	Laboratory measurement	HBT	NA	0.307	[84]
2018	A wood panel envelope; a modular plywood panel envelope	In situ measurement	HFM	0.150 0.154	0.174 (in winter) 0.201 (in winter)	[52]
2020	CLT envelopes	Laboratory measurement	HBT	0.16 0.15	0.148 0.199	[81]
2020	Timber envelopes	In situ measurement	HFM	0.50	0.60–0.65	[88]
2021	A four-layered spruce wood envelope	Laboratory measurement	HBT	NA	0.375	[89]
2021	3 types of wood-framed envelopes with different structures	In situ measurement	QIRT	0.23 0.16 0.16	0.09–0.25 0.04–0.21 0.20–0.26	[90]
2022	4 types of wood-framed envelopes with different structures	In situ measurement	QIRT	NA	0.43 0.31 0.26 0.24	[32]

2.4. Straw Bale Envelopes

Although straw bale has been used widely as a construction material since the 20th century, the benefits of this material have been recognised in the last decade. The notable advantages are impressive physical properties, including thermal and acoustic insulation, an energy-efficient manufacturing process and a carbon storage capacity [91–93]. In recent years, more researchers have focused on the U-values of straw bale envelopes. In related studies, the most common structure of straw bale envelopes is the straw bale envelope with a timber frame, as shown in Table 4. An alternative to this is a metal frame structure, such as a light-gauge steel frame [94]. There are also many different types of straw, such as wheat straw, rice straw, oat straw and corn straw.

There is limited research on the theoretical U-values for straw bale envelopes. In existing studies, Miljan et al. studied the theoretical and measured U-values of a straw bale envelope [95]. The results showed that the measured U-value (0.125 W/m²K) differed from the theoretical U-value, which was 0.092 W/m²K. As a new building envelope type, there is limited information related to the thermal conductivity of different straw bales. Thus, it is difficult to calculate theoretical U-values of straw bale envelopes with different structures and materials. More quantitative research on the thermal conductivity of different straw bales needs to be conducted to fill this research gap in the future.

Most studies have focused on the measured U-values for straw bale envelopes. Laboratory measurements were applied in the majority of these with the remainder applying in situ measurements. The measured U-values range from 0.12 to 1.30 W/m²K with most concentrated around 0.2 W/m²K. The wide range of measured U-values may be related to the envelope materials. For example, Sun et al. applied the CHB method to explore the measured U-values of the straw bale envelopes with light-gauge steel frames. The results showed the measured U-value of the envelope with the paper straw board (0.669 W/m²K) was lower than that with the wheat straw strand board (0.912 W/m²K) [94].

Table 4. Existing studies related to U-values of straw bale envelopes.

Year	Envelope Type	Measurement Type	Measurement Method	Theoretical U-Value (W/m²·K)	Measured U-Value (W/m²·K)	Reference
2015	A straw bale envelope with a timer frame	In situ measurement	HFM	0.092	0.125	[95]
2016	A straw bale envelope with a timer frame	Laboratory measurement	CHB	NA	0.20 ± 0.016	[96]
2017	Two straw bale envelopes with timber frames	In situ measurement	HFM	NA	0.119 ± 0.041 (in winter) 0.253 ± 0.085 (in winter)	[97]
2018	Straw envelopes with timber frames	NA	NA	0.72	NA	[98]
2019	A straw bale envelope with a timber frame	Laboratory measurement	HBT	NA	0.281	[99]
2020	A multi-sheet straw bale envelope with a timber frame	Laboratory measurement	HBT	NA	0.154	[100]
2021	Straw bale envelopes with plywood frames	In situ measurement	THM	NA	0.3–1.3	[101]
2021	Straw bale envelopes with different structures	Laboratory measurement	GHB	NA	0.48–0.53	[16]
2023	Light-gauge steel-framed straw envelopes	Laboratory measurement	CHB	NA	0.661–0.912	[94]

Figure 2 summarises the theoretical and measured U-values for four types of envelopes in Tables 1–4. Compared with inorganic envelopes, bio-based envelopes have lower U-values, and the differences between the measured and theoretical U-values of bio-based envelopes are smaller. It indicates that the thermal performances of bio-based envelopes are close to expectations. However, related data are not sufficient. More related measurements need to be conducted in the future. Among the two types of inorganic envelopes, the ranges of both theoretical and measured U-values are large for brick envelopes due to the greater variety of brick envelopes. Concrete envelopes have a small range of theoretical U-values and a large range of measured U-values, suggesting that the actual insulation performances of concrete envelopes may be lower than expected.
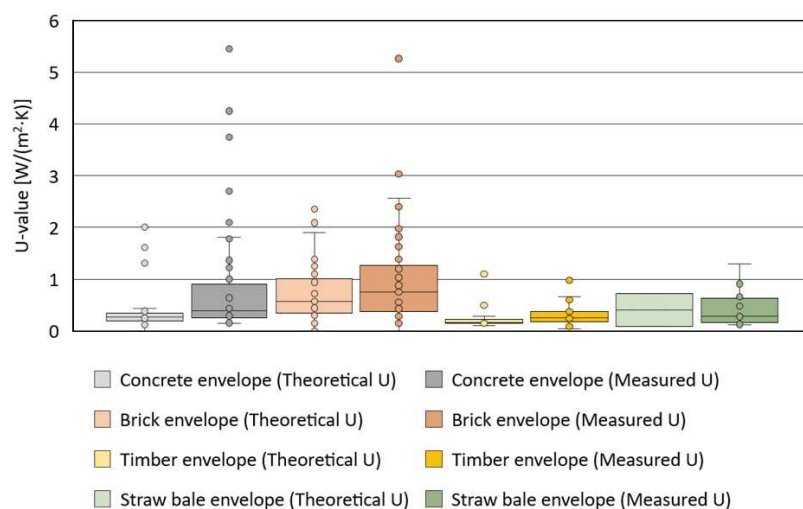
Figure 2. Theoretical and measured U-value distribution of four types of envelopes.

3. Environmental Factors Influencing U-Values

As the U-value represents the heat transfer capacity of the envelope in the actual environment, the environmental factors influencing the U-value are complex. The main environmental factors include temperature, relative humidity and solar radiation. There is limited research on the factors influencing U-values, and there is a positive correlation between the U-value of the envelope and the thermal conductivity of the envelope material. This section will also summarise articles related to the thermal conductivities of building materials, as shown in Table 5.

The thermal conductivities of building materials can be affected by changes in the thermal conductivities of air and water due to temperature changes. When temperature increases from 10 to 40 °C, air and water conductivities will increase by 10% and 8%, respectively. Regarding the high amount of air with water vapour in the envelopes, the increase in air and water conductivities is not negligible. Existing studies have quantified the effects of temperature on the thermal conductivities of both conventional and bio-based building materials. Wang studied the thermal conductivity of aerogel-incorporated concrete (AIC). The results indicated that the thermal conductivity of AIC increased by 15.5% from 20 to 90 °C [102]. Danovska studied dynamic thermal conductivity functions dependent on temperature for some timber materials. The results indicated that the thermal conductivities of CLT, woodchips, and wood–fibre panels increased 10.2%, 26%, and 21% from 10 to 50 °C [103]. However, there is limited research examining the quantitative relationship between temperature and the U-values of various envelopes.

In terms of relative humidity effects, relative humidity can change the moisture contents of building materials, affecting the thermal conductivities of building materials and thus the U-values of envelopes. The moisture content of a building material in an actual situation is related to its hygroscopicity, which is mainly related to the composition, porosity and pore characteristics. Several studies have quantified the effects of relative humidity and moisture contents on the thermal conductivity of building materials and U-values of envelopes [104]. Various types of building materials and envelopes are studied. There is more research on insulation materials. This may be because insulation materials are usually porous, and their thermal conductivities are more susceptible to the effects of relative humidity. For example, Wang et al. investigated the relationship between the relative humidity and the thermal conductivity of common insulation materials. The result showed that the thermal conductivities of these materials increased by more than 100% when relative humidity increased from 0% to 100% [105]. Boukhattem et al. analysed the influence of moisture content on the thermal conductivity of the date palm fibre (DPF) insulation board. The result showed that the thermal conductivity of the DPF board could increase four times from a dry stage to its saturation state [106].

In addition, solar radiation is also a factor influencing U-values. It has been found that solar radiation can increase the heat flow through envelopes and thus increase the U-values of the envelopes. Evangelisti et al. conducted in situ U-value measurements in both summer and winter in Italy. As the building being tested was located in the northern hemisphere, the solar radiation intensity and sunlight hours were higher on the south envelope than on the north envelope. The results showed that the U-values of the south envelope were approximately 25% higher than the U-values of the north envelope in both winter and summer [23]. Ahmad et al. also found that the U-values of the east envelope were approximately 23% higher than the U-values of the north envelope in Saudi Arabia [45]. This is because the north envelope is exposed to solar radiation for a shorter time than the east envelope, which leads to a lower heat flow through the north envelope. However, limited studies have been conducted to quantify the relationship between U-values and solar radiation. This needs to be systematically studied in the future.

Table 5. Environmental factors influencing U-values of envelopes.

Factors	Year	Building Material	Influence	Reference
Temperature	2016	Hemp concrete, flax concrete and rape straw concrete	The thermal conductivity increases by approximately 10% for hemp and flax and 18% for rape straw from 10 to 40 °C.	[107]
	2019	AIC with different aerogel volume admixtures	The thermal conductivity increases by 15.5% from 20 to 90 °C.	[102]
	2022	Common insulation materials	The thermal conductivity increases by 12.6% from 20 to 60 °C.	[105]
	2022	CLT panels; woodchip insulation panels; wood–fibre insulation panels	The thermal conductivity increases by 10.2% for CLT, 26% for woodchips and 21% for wood–fibre from 10 to 50 °C.	[103]
Relative humidity	2012	Mineral wools	The thermal conductivity increases from 0.10–0.14 W/m K to 0.7–0.9 W/m K (from low moisture contents of 5–20% to saturation).	[104]
	2014	Stone wool panels; hemp panels	U-values of both stone wool panels and hemp panels increase in 56–90% RH.	[86]
	2016	Hemp concrete, flax concrete and rape straw concrete	The thermal conductivity is proportional to the water content.	[107]
	2016	Solid brick envelopes	The transient U-values achieve higher values within the moist stage.	[108]
	2017	Insulating building materials made from DPF mesh	Thermal conductivity increases with water content.	[105]
	2019	AIC with aerogel volume admixtures	The thermal conductivity increases by 76.33% from 0% to 100% RH.	[102]
	2022	Common insulation materials	The thermal conductivity increases by 171.9% from 0% to 100% RH.	[105]
	2022	CLT panels; woodchip insulation panels; wood–fibre insulation panels	The thermal conductivity increases by 12% for CLT, 18% for woodchips and 8% for wood–fibre from low to high moisture content.	[103]
Solar radiation	2014	Hollow-reinforced precast concrete envelopes	The U-value of the north envelope was 37.3% lower than that of the east envelope, because the north envelope was exposed to solar radiation for a shorter time than the east envelope.	[45]
	2020	RC envelopes	The obtained U-value can be heightened by solar radiation.	[23]

4. Impacts of U-Values on Building Energy Consumption

The life cycle energy of buildings includes embodied energy and operational energy, as shown in Figure 3. As an important thermal parameter of the envelope, the U-value affects the building's operational energy, especially energy consumption for cooling and heating. In recent years, the number of studies on the relationship between operational energy consumption and U-values of envelopes has increased rapidly, as shown in Table 6. The types of buildings in these studies are mainly office and residential buildings. The types of envelopes examined include inorganic envelopes (such as concrete envelopes and brick envelopes) and bio-based envelopes (such as timber envelopes and straw bale envelopes).

According to existing studies, the U-values have a large impact on building operational energy consumption, and the relationship between the U-value and operational energy consumption varies in different climatic conditions. Lower U-values can save operational energy in cold climates. For example, Fernandes et al. used dynamic simulation to study the U-value impact on the thermal performance of residential buildings. The results showed that operational energy consumption decreased as U-values decreased in cold climates [109]. However, the relationship between U-values and operational energy consumption needs to be dependent on the specific situations in relatively warm climates. On the one hand, some researchers have found that lower U-values can lead to higher operational energy

consumption. For example, Ihara et al. investigated envelope properties in their study of energy efficiency in Tokyo office buildings. The results showed that the decrease in the U-value of the non-transparent parts of RC envelopes was observed to increase the yearly energy use of some high-rise buildings [110]. On the other hand, some researchers have reached the opposite conclusion. For example, Suleiman found that when U-values of external envelopes are 3.03 W/m^{2}k and 5.26 W/m^{2}k, the corresponding estimated annual energy consumption is 40.26 kWh/m^2 and 69.93 kWh/m^2 in North Africa [64].
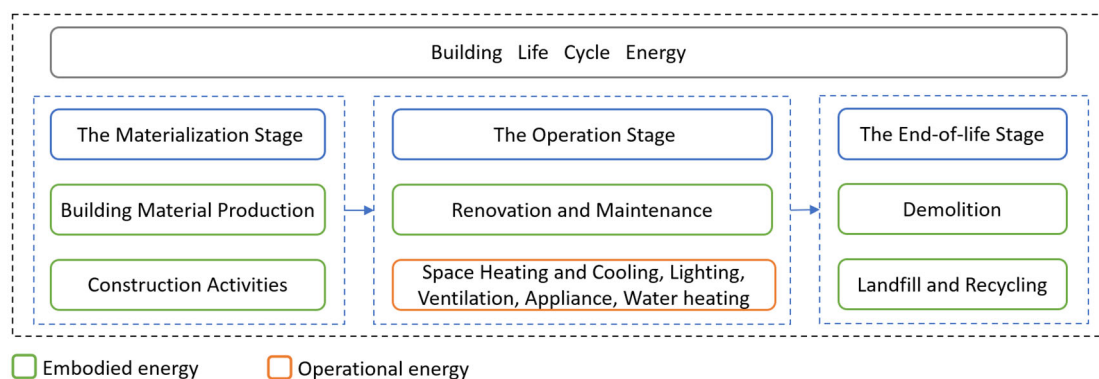

Figure 3. The life cycle energy of buildings.

Table 6. Impacts of U-values of envelopes on building energy consumption.

Year	Building Use	Envelope Type	Influence on Energy Consumption	Reference
2006	All use	The breathing envelope	This envelope achieves ultra-low U-values. It is responsible for a 10% reduction in space heating and cooling energy.	[111]
2011	All use	Concrete-backed stone masonry envelope	When U-values of external envelopes are 3.03 W/(m^2·K) and 5.26 W/(m^2·K), the corresponding estimated annual energy consumption are 40.26 kWh/m^2 and 69.93 kWh/m^2 in North Africa.	[64]
2012	All use	Timber envelopes	There is a linear relationship between the average U-value of the envelope and the cooling and heating energy consumption.	[112]
2015	Office	RC envelopes	The energy use decreased due to the reduction in the U-values of windows. The energy use increased due to the reduction in the U-value of the non-transparent envelopes in high-rise buildings.	[110]
2015	Residential	RC envelopes	In cold areas, the yearly heating energy use of buildings modelled with the 3D dynamic method is 8–13% higher than that modelled with the average method. In warm areas, the yearly cooling energy use is underestimated by 17% with the average method.	[113]
2016	Residential	RC envelopes	The equivalent U-value method underestimates heating energy use by up to 15%.	[114]
2016	Residential	Straw bale envelopes	Straw bale envelopes have a lower U-value than traditional building materials and are more energy efficient in Estonia.	[96]
2016	Residential	NA	The variability of U-values can underestimate the energy performance of approximately 90% of residences.	[115]
2017	Residential	Concrete block envelopes	The average U-value method underestimates yearly heating energy consumption by 13%.	[116]

Table 6. *Cont.*

Year	Building Use	Envelope Type	Influence on Energy Consumption	Reference
2018	All use	RC, brick, CLT, and timber-frame envelopes	The U-values of building components impact the energy performance of building components significantly.	[117]
2018	Office	NA	In the hot–arid climate zone, U-values of the envelopes do not impact energy performance significantly.	[118]
2018	Residential	NA	Low U-values can increase building energy demand in temperate regions.	[119]
2019	All use	NA	In cold areas, building energy consumption decreased due to the reduction in U-values. In warmer climates, low U-values building increased energy consumption.	[109]
2021	All use	Straw bale envelopes	The theoretical U-value of the straw bale envelope is $0.13 \text{ W}/(\text{m}^2 \cdot \text{K})$. The heat load loss is from 18% to 25%, while heat load gain is from 3% to 10% in the whole building.	[91]
2022	Residential	Straw bale envelopes	The U-value of straw bale envelope is $0.1 \text{ W}/(\text{m}^2 \cdot \text{K})$, the U-value of the conventional envelope is $2.6 \text{ W}/(\text{m}^2 \cdot \text{K})$. Straw bale reduced energy consumption in all climates except for the warm–humid one in Iran.	[40]
2022	Residential	Brick and concrete envelopes	Due to the variation in U-value, the yearly total heating load increased by 26%, and the yearly total cooling load increased by 13% in Beijing.	[120]
2022	All use	Brick and concrete envelopes	In the Mediterranean climate, the change in U-value each month is significant, providing deviances as much as 9.2% in quarterly energy consumption.	[12]

The fluctuation of U-values can also have impacts on the predictions of building operational energy consumption. U-values are dynamic because they are influenced by environmental factors, such as fluctuations in temperature and relative humidity. If an average U-value or a theoretical U-value is used to simulate building operational energy consumption throughout the year, errors will arise. Bruno et al. applied the WUFI software to study dynamic U-values of three different inorganic envelopes in the Mediterranean climate. The results showed that the changes in the U-values each month were significant, providing deviances of as much as 9.2% in quarterly energy consumption when compared to the results obtained from a steady-state U-value [12]. The fluctuation of U-values is an important issue for building energy prediction. However, related quantitative research focusing on bio-based building envelopes is limited and needs to be investigated in detail.

5. Comparison of Theoretical and Measured U-Values

In recent years, many countries have established the range of U-values of envelopes in building codes to save building energy use [121–123]. The U-values in these codes are theoretical U-values. More existing studies have used theoretical U-values, and fewer studies have applied measured U-values to simulate building operational energy. To predict building operational energy accurately, it is important to obtain U-values of envelopes in actual situations, so it is vital to understand whether the theoretical and measured U-values correspond to the real-life scenario.

Firstly, theoretical U-values of envelopes are different from actual situations of envelopes in most situations because they can be affected by environmental factors, especially temperature and relative humidity. The temperature and relative humidity are constantly varying in the real environment. Several researchers have focused on dynamic U-values [124–126]. Their findings suggest that using theoretical U-values for building energy simulation may lead to errors to some extent.

Secondly, whether the measured U-values are close to the actual conditions of envelopes needs to be verified. Lots of research results showed that the theoretical U-values of both inorganic and bio-based envelopes were different from their measured U-values. The measured U-values may be closer to the actual situations of envelopes than the theoretical U-values because the measured U-values take the influence of the environment into account. However, errors in measured U-values may be caused by incorrect installation of equipment and unstable measurement conditions [127]. Thus, it cannot be stated conclusively that the measured U-values correspond to the actual situations of envelopes. It is worth noting that most of the existing studies do not verify the measured U-values.

6. Conclusions

This study provides a systematic review of the existing studies related to the U-values for envelopes of different materials. Both theoretical and measured U-values of four types of envelopes (including concrete, brick, timber and straw bale envelopes) are introduced. Environmental factors influencing U-values and the impacts of U-values on building energy consumption are analysed. This study also discusses the accuracy of both theoretical and measured U-values. Three research findings are summarised as follows:

(1) The relationship between environmental factors and U-values needs to be studied in detail. Some studies have focused on the relationship between the environmental factors and thermal conductivities of building materials. However, there is limited research examining the quantitative relationship between important factors (such as temperature, relative humidity and solar radiation) and the U-values of various envelopes.

(2) The gaps between theoretical and measured U-values are significant, especially for concrete and brick envelopes. The theoretical U-values of concrete envelopes range from 0.12 to 1.61 W/m^{2}K. Meanwhile, the measured U-values of concrete envelopes range from 0.14 to 5.45 W/m^{2}K. The theoretical U-values of brick envelopes range from 0.22 to 2.09 W/m^{2}K. Meanwhile, the measured U-values of brick envelopes range from 0.15 to 5.26 W/m^{2}K.

(3) The accuracy of both theoretical and the measured U-values needs to be verified. In building energy simulation, it is also necessary to verify which type of U-value to input can make the simulation results more accurate.

Conflicts of Interest: The authors declare no conflicts of interest.

Abbreviations

Nomenclature

U	Thermal transmittance $[\text{W}/(\text{m}^2 \cdot \text{K})]$
Φ	Heat tranfer [W]
A	Area $[\text{m}^2]$
ΔT	Temperature difference between the interior and exterior sides of the building envelope [K]
R	Thermal resistance $[(\text{m}^2 \cdot \text{K})/\text{W}]$
D	Thickness of the material [mm]
λ	Thermal conductivity of the material $[\text{W}/(\text{m} \cdot \text{K})]$
HBT	Hot Box Test
GHB	Guarded hot box
CHB	Calibrated hot box
q	Heat flow density $[\text{W}/\text{m}^2]$
T	Temperature [K]
HFM	Heat flow meter
SHB-HFM	Simple hot box-heat flow meter
THM	Thermometric

QIRT	Quantitative infrared thermography
h	Heat transfer coefficient $[\mathrm{W}/(\mathrm{m}^2{\cdot}\mathrm{K})]$
LCA	Life cycle assessment
RC	Reinforced concrete
CLT	Cross-laminated timber
OSB	Oriented strand board
AIC	Aerogel-incorporated concrete
Subscripts	
sum	Sum of all layers within the envelope
se	External surface of the envelope
si	Internal surface of the envelope
ij	Indoor environment at time j
ej	Outdoor environment at time j
n	The number of recorded samples during the measurement period
sij	Internal surface of the envelope at time j
i	Internal surface of the envelope

References

1. Lee, J.; Kim, J.; Song, D.; Kim, J.; Jang, C. Impact of external insulation and internal thermal density upon energy consumption of buildings in a temperate climate with four distinct seasons. *Renew. Sustain. Energy Rev.* **2017**, *75*, 1081–1088. [CrossRef]
2. Almasri, R.A.; Alshitawi, M.S. Electricity consumption indicators and energy efficiency in residential buildings in GCC countries: Extensive review. *Energy Build.* **2022**, *255*, 111664. [CrossRef]
3. Zhu, S.; Causone, F.; Gao, N.; Ye, Y.; Jin, X.; Zhou, X.; Shi, X. Numerical simulation to assess the impact of urban green infrastructure on building energy use: A review. *Build. Environ.* **2023**, *228*, 109832. [CrossRef]
4. Nematchoua, M.K.; Sendrahasina, R.M.; Malmedy, C.; Orosa, J.A.; Simo, E.; Reiter, S. Analysis of environmental impacts and costs of a residential building over its entire life cycle to achieve nearly zero energy and low emission objectives. *J. Clean. Prod.* **2022**, *373*, 133834. [CrossRef]
5. Wang, P.; Yang, Y.; Ji, C.; Huang, L. Positivity and difference of influence of built environment around urban park on building energy consumption. *Sustain. Cities Soc.* **2023**, *89*, 104321. [CrossRef]
6. Ni, S.; Zhu, N.; Hou, Y.; Zhang, Z. Research on indoor thermal comfort and energy consumption of zero energy wooden structure buildings in severe cold zone. *J. Build. Eng.* **2023**, *67*, 105965. [CrossRef]
7. Dougherty, T.R.; Jain, R.K. Invisible walls: Exploration of microclimate effects on building energy consumption in New York City. *Sustain. Cities Soc.* **2023**, *90*, 104364. [CrossRef]
8. Moradi, A.; Kavgic, M.; Costanzo, V.; Evola, G. Impact of typical and actual weather years on the energy simulation of buildings with different construction features and under different climates. *Energy* **2023**, *270*, 126875. [CrossRef]
9. Catto Lucchino, E.; Gennaro, G.; Favoino, F.; Goia, F. Modelling and validation of a single-storey flexible double-skin façade system with a building energy simulation tool. *Build. Environ.* **2022**, *226*, 109704. [CrossRef]
10. Guarino, F.; Tumminia, G.; Longo, S.; Cellura, M.; Cusenza, M.A. An integrated building energy simulation early—Design tool for future heating and cooling demand assessment. *Energy Rep.* **2022**, *8*, 10881–10894. [CrossRef]
11. Klemp, S.; Abida, A.; Richter, P. A method and analysis of predicting building material U-value ranges through geometrical pattern clustering. *J. Build. Eng.* **2021**, *44*, 103243. [CrossRef]
12. Bruno, R.; Bevilacqua, P. Heat and mass transfer for the U-value assessment of opaque walls in the Mediterranean climate: Energy implications. *Energy* **2022**, *261*, 124894. [CrossRef]
13. *ISO 6946:2007*; Building Components and Building Elements—Thermal Resistance and Thermal Transmittance—Calculation Method. International Standard ISO: Geneva, Switzerland, 2007.
14. *ASTM C1363-05*; Standard Test Method for Thermal Performance of Building Materials and Envelope Assemblies by Means of a Hot Box Apparatus. American Society for Testing and Materials: West Conshohocken, PA, USA, 2005.
15. *EN ISO 8990*; Thermal Insulation—Determination of Steady-State Thermal Transmission Properties—Calibrated and Guarded Hot Box. European Standard: Lausanne, Switzerland, 1996.
16. Yang, L.; Yang, J.; Liu, Y.; An, Y.; Chen, J. Hot box method to investigate U-values for straw bale walls with various structures. *Energy Build.* **2021**, *234*, 110706. [CrossRef]
17. Nardi, I.; Paoletti, D.; Ambrosini, D.; de Rubeis, T.; Sfarra, S. U-value assessment by infrared thermography: A comparison of different calculation methods in a Guarded Hot Box. *Energy Build.* **2016**, *122*, 211–221. [CrossRef]
18. Asdrubali, F.; Baldinelli, G. Thermal transmittance measurements with the hot box method: Calibration, experimental procedures, and uncertainty analyses of three different approaches. *Energy Build.* **2011**, *43*, 1618–1626. [CrossRef]
19. Chen, F.; Wittkopf, S.K. Summer condition thermal transmittance measurement of fenestration systems using calorimetric hot box. *Energy Build.* **2012**, *53*, 47–56. [CrossRef]
20. *ISO 9869-1*; Thermal Insulation, Building Elements, In-Situ Measurement of Thermal Resistance and Thermal Transmittance—Part 1: Heat Flow Meter Method. International Standard ISO: Geneva, Switzerland, 2014.

21. *ASTM C1155-95*; Standard, Standard Practice for Determining Thermal Resistance of Building Envelope Components from the In-situ Data. American Society for Testing and Materials: West Conshohocken, PA, USA, 2007.

22. Gumbarević, S.; Milovanović, B.; Bašić, B.D.; Gaši, M. Combining Deep Learning and the Heat Flux Method for In-Situ Thermal-Transmittance Measurement Improvement. *Energies* **2022**, *15*, 5029. [CrossRef]

23. Evangelisti, L.; Guattari, C.; Vollaro, R.D.L.; Asdrubali, F. A methodological approach for heat-flow meter data post-processing under different climatic conditions and wall orientations. *Energy Build.* **2020**, *223*, 110216. [CrossRef]

24. Gaspar, K.; Casals, M.; Gangolells, M. In situ measurement of façades with a low U-value: Avoiding deviations. *Energy Build.* **2018**, *170*, 61–73. [CrossRef]

25. Ficco, G.; Guattari, C.; Vollaro, R.D.L.; Asdrubali, F. U-value in situ measurement for energy diagnosis of existing buildings. *Energy Build.* **2015**, *104*, 108–121. [CrossRef]

26. Meng, X.; Gao, Y.; Wang, Y.; Yan, B.; Zhang, W.; Long, E. Feasibility experiment on the simple hot box-heat flow meter method and the optimization based on simulation reproduction. *Appl. Therm. Eng.* **2015**, *83*, 48–56. [CrossRef]

27. Bienvenido-Huertas, D.; Rodríguez-Álvaro, R.; Moyano, J.J.; Rico, F.; Marín, D. Determining the U-Value of Façades Using the Thermometric Method: Potentials and Limitations. *Energies* **2018**, *11*, 360. [CrossRef]

28. *ISO 9869-2*; Thermal Insulation—Building Elements—In-Situ Measurement of Thermal Resistance and Thermal Transmittance—Part 2: Infrared Method for Frame Structure Dwelling. International Standard ISO: Geneva, Switzerland, 2018.

29. *ASTM C1060*; Standard Practice for Thermographic Inspection of Insulation Installations in Envelope Cavities of Frame Buildings. American Society for Testing and Materials: West Conshohocken, PA, USA, 2011.

30. Teni, M.; Krstić, H.; Kosiński, P. Review and comparison of current experimental approaches for in-situ measurements of building walls thermal transmittance. *Energy Build.* **2019**, *203*, 109417. [CrossRef]

31. Tardy, F. A review of the use of infrared thermography in building envelope thermal property characterization studies. *J. Build. Eng.* **2023**, *75*, 106918. [CrossRef]

32. Mahmoodzadeh, M.; Gretka, V.; Lee, I.; Mukhopadhyaya, P. Infrared thermography for quantitative thermal performance assessment of wood-framed building envelopes in Canada. *Energy Build.* **2022**, *258*, 111807. [CrossRef]

33. O'Hegarty, R.; Kinnane, O.; Lennon, D.; Colclough, S. In-situ U-value monitoring of highly insulated building envelopes: Review and experimental investigation. *Energy Build.* **2021**, *252*, 111447. [CrossRef]

34. Papadakos, G.; Marinakis, V.; Konstas, C.; Doukas, H.; Papadopoulos, A. Managing the uncertainty of the U-value measurement using an auxiliary set along with a thermal camera. *Energy Build.* **2021**, *242*, 110984. [CrossRef]

35. Krstić, H.; Miličević, I.; Markulak, D.; Domazetović, M. Thermal Performance Assessment of a Wall Made of Lightweight Concrete Blocks with Recycled Brick and Ground Polystyrene. *Buildings* **2021**, *11*, 584. [CrossRef]

36. Li, H.; Li, Y.; Wang, Z.; Shao, S.; Deng, G.; Xue, H.; Xu, Z.; Yang, Y. Integrated building envelope performance evaluation method towards nearly zero energy buildings based on operation data. *Energy Build.* **2022**, *268*, 112219. [CrossRef]

37. Guo, Y.-Y. Revisiting the building energy consumption in China: Insights from a large-scale national survey. *Energy Sustain. Dev.* **2022**, *68*, 76–93. [CrossRef]

38. Ninikas, K.; Tallaros, P.; Mitani, A.; Koutsianitis, D.; Ntalos, G.; Taghiyari, H.R.; Papadopoulos, A.N. Thermal Behavior of a Light Timber-Frame Wall vs. a Theoretical Simulation with Various Insulation Materials. *J. Compos. Sci.* **2022**, *6*, 22.

39. Evola, G.; Costanzo, V.; Urso, A.; Tardo, C.; Margani, G. Energy performance of a prefabricated timber-based retrofit solution applied to a pilot building in Southern Europe. *Build. Environ.* **2022**, *222*, 109442. [CrossRef]

40. Mehravar, M.; Veshkini, A.; Veiseh, S.; Fayaz, R. Physical properties of straw bale and its effect on building energy conservation and carbon emissions in different climatic regions of Iran. *Energy Build.* **2022**, *254*, 111559. [CrossRef]

41. Zhou, Y.; Trabelsi, A.; El Mankibi, M. A review on the properties of straw insulation for buildings. *Constr. Build. Mater.* **2022**, *330*, 127215. [CrossRef]

42. Andersen, J.H.; Rasmussen, N.L.; Ryberg, M.W. Comparative life cycle assessment of cross laminated timber building and concrete building with special focus on biogenic carbon. *Energy Build.* **2022**, *254*, 111604. [CrossRef]

43. Hawkins, W.; Cooper, S.; Allen, S.; Roynon, J.; Ibell, T. Embodied carbon assessment using a dynamic climate model: Case-study comparison of a concrete, steel and timber building structure. *Structures* **2021**, *33*, 90–98. [CrossRef]

44. Li, H.; Luo, Z.; Xu, X.; Cang, Y.; Yang, L. Assessing the embodied carbon reduction potential of straw bale rural houses by hybrid life cycle assessment: A four-case study. *J. Clean. Prod.* **2021**, *303*, 127002. [CrossRef]

45. Ahmad, A.; Maslehuddin, M.; Al-Hadhrami, L.M. In situ measurement of thermal transmittance and thermal resistance of hollow reinforced precast concrete walls. *Energy Build.* **2014**, *84*, 132–141. [CrossRef]

46. Nussbaumer, T.; Wakili, K.G.; Tanner, C. Experimental and numerical investigation of the thermal performance of a protected vacuum-insulation system applied to a concrete wall. *Appl. Energy* **2006**, *83*, 841–855. [CrossRef]

47. Asdrubali, F.; D'alessandro, F.; Baldinelli, G.; Bianchi, F. Evaluating in situ thermal transmittance of green buildings masonries—A case study. *Case Stud. Constr. Mater.* **2014**, *1*, 53–59. [CrossRef]

48. Mandilaras, I.; Atsonios, I.; Zannis, G.; Founti, M. Thermal performance of a building envelope incorporating ETICS with vacuum insulation panels and EPS. *Energy Build.* **2014**, *85*, 654–665. [CrossRef]

49. Samardzioska, T.; Apostolska, R. Measurement of Heat-Flux of New Type Façade Walls. *Sustainability* **2016**, *8*, 1031. [CrossRef]

50. Caruana, C.; Yousif, C.; Bacher, P.; Buhagiar, S.; Grima, C. Determination of thermal characteristics of standard and improved hollow concrete blocks using different measurement techniques. *J. Build. Eng.* **2017**, *13*, 336–346. [CrossRef]

51. Choi, D.S.; Ko, M.J. Comparison of Various Analysis Methods Based on Heat Flowmeters and Infrared Thermography Measurements for the Evaluation of the In Situ Thermal Transmittance of Opaque Exterior Walls. *Energies* **2017**, *10*, 1019. [CrossRef]

52. Ratnieks, J.; Jakovics, A.; Gendelis, S. Wall assemblies U-value calculation in test buildings using constant power heating. *Energy Procedia* **2018**, *147*, 207–213. [CrossRef]

53. Tejedor, B.; Casals, M.; Macarulla, M.; Giretti, A. U-value time series analyses: Evaluating the feasibility of in-situ short-lasting IRT tests for heavy multi-leaf walls. *Build. Environ.* **2019**, *159*, 106123. [CrossRef]

54. Tejedor, B.; Barreira, E.; de Freitas, V.P.; Kisilewicz, T.; Nowak-Dzieszko, K.; Berardi, U. Impact of Stationary and Dynamic Conditions on the U-Value Measurements of Heavy-Multi Leaf Walls by Quantitative IRT. *Energies* **2020**, *13*, 6611. [CrossRef]

55. O'Hegarty, R.; Reilly, A.; West, R.; Kinnane, O. Thermal investigation of thin precast concrete sandwich panels. *J. Build. Eng.* **2020**, *27*, 100937. [CrossRef]

56. Huang, B.; Lu, W. Experimental Investigation of the Multi-Physical Properties of an Energy Efficient Translucent Concrete Panel for a Building Envelope. *Appl. Sci.* **2020**, *10*, 6863. [CrossRef]

57. Sun, J.; Xiao, J.; Li, Z.; Feng, X. Experimental study on the thermal performance of a 3D printed concrete prototype building. *Energy Build.* **2021**, *241*, 110965. [CrossRef]

58. Lee, Y.-J.; Moon, J.-H.; Choi, D.-S.; Ko, M.-J. Application of the Heat Flow Meter Method and Extended Average Method to Improve the Accuracy of In Situ U-Value Estimations of Highly Insulated Building Walls. *Sustainability* **2024**, *16*, 5687. [CrossRef]

59. Calis, M. Change of U-value with extreme temperatures on different types of block walls. *J. Build. Eng.* **2024**, *85*, 108653. [CrossRef]

60. Albatici, R.; Tonelli, A.M. Infrared thermovision technique for the assessment of thermal transmittance value of opaque building elements on site. *Energy Build.* **2010**, *42*, 2177–2183. [CrossRef]

61. Marshall, A.; Francou, J.; Fitton, R.; Swan, W.; Owen, J.; Benjaber, M. Variations in the U-Value Measurement of a Whole Dwelling Using Infrared Thermography under Controlled Conditions. *Buildings* **2018**, *8*, 46. [CrossRef]

62. Evangelisti, L.; Guattari, C.; Gori, P.; Vollaro, R.D.L. In Situ Thermal Transmittance Measurements for Investigating Differences between Wall Models and Actual Building Performance. *Sustainability* **2015**, *7*, 10388–10398. [CrossRef]

63. Ghazi Wakili, K.; Tanner, C. U-value of a dried wall made of perforated porous clay bricks: Hot box measurement versus numerical analysis. *Energy Build.* **2003**, *35*, 675–680. [CrossRef]

64. Suleiman, B.M. Estimation of U-value of traditional North African houses. *Appl. Therm. Eng.* **2011**, *31*, 1923–1928. [CrossRef]

65. Fokaides, P.A.; Kalogirou, S.A. Application of infrared thermography for the determination of the overall heat transfer coefficient (U-Value) in building envelopes. *Appl. Energy* **2011**, *88*, 4358–4365. [CrossRef]

66. Naveros, I.; Jiménez, M.J.; Heras, M.R. Analysis of capabilities and limitations of the regression method based in averages, applied to the estimation of the U value of building component tested in Mediterranean weather. *Energy Build.* **2012**, *55*, 854–872. [CrossRef]

67. Morales, M.P.; Juárez, M.; Muñoz, P.; Mendívil, M.; Ruiz, J. Possibilities for improving the equivalent thermal transmittance of single-leaf walls for buildings. *Energy Build.* **2014**, *69*, 473–480. [CrossRef]

68. Albatici, R.; Tonelli, A.M.; Chiogna, M. A comprehensive experimental approach for the validation of quantitative infrared thermography in the evaluation of building thermal transmittance. *Appl. Energy* **2015**, *141*, 218–228. [CrossRef]

69. Walker, R.; Pavía, S. Thermal performance of a selection of insulation materials suitable for historic buildings. *Build. Environ.* **2015**, *94*, 155–165. [CrossRef]

70. Santos, P.; Martins, C.; Júlio, E. Enhancement of the thermal performance of perforated clay brick walls through the addition of industrial nano-crystalline aluminium sludge. *Constr. Build. Mater.* **2015**, *101*, 227–238. [CrossRef]

71. Pavlík, Z.; Jerman, M.; Fořt, J.; Černý, R. Monitoring Thermal Performance of Hollow Bricks with Different Cavity Fillers in Difference Climate Conditions. *Int. J. Thermophys.* **2015**, *36*, 557–568. [CrossRef]

72. Litti, G.; Khoshdel, S.; Audenaert, A.; Braet, J. Hygrothermal performance evaluation of traditional brick masonry in historic buildings. *Energy Build.* **2015**, *105*, 393–411. [CrossRef]

73. Gaspar, K.; Casals, M.; Gangolells, M. A comparison of standardized calculation methods for in situ measurements of façades U-value. *Energy Build.* **2016**, *130*, 592–599. [CrossRef]

74. Evangelisti, L.; Guattari, C.; Gori, P.; Vollaro, R.d.L.; Asdrubali, F. Experimental investigation of the influence of convective and radiative heat transfers on thermal transmittance measurements. *Int. Commun. Heat Mass Transf.* **2016**, *78*, 214–223. [CrossRef]

75. Campbell, N.; McGrath, T.; Nanukuttan, S.; Brown, S. Monitoring the hygrothermal and ventilation performance of retrofitted clay brick solid wall houses with internal insulation: Two UK case studies. *Case Stud. Constr. Mater.* **2017**, *7*, 163–179. [CrossRef]

76. Lucchi, E. Thermal transmittance of historical brick masonries: A comparison among standard data, analytical calculation procedures, and in situ heat flow meter measurements. *Energy Build.* **2017**, *134*, 171–184. [CrossRef]

77. Rotilio, M.; Cucchiella, F.; De Berardinis, P.; Stornelli, V. Thermal Transmittance Measurements of the Historical Masonries: Some Case Studies. *Energies* **2018**, *11*, 2987. [CrossRef]

78. Mouton, L.; Allacker, K.; Röck, M. Bio-based building material solutions for environmental benefits over conventional construction products—Life cycle assessment of regenerative design strategies (1/2). *Energy Build.* **2023**, *282*, 112767. [CrossRef]

79. Mouton, L.; Cucchiella, F.; De Berardinis, P.; Stornelli, V. Low-tech passive solar design concepts and bio-based material solutions for reducing life cycle GHG emissions of buildings—Life cycle assessment of regenerative design strategies (2/2). *Energy Build.* **2023**, *282*, 112678. [CrossRef]

80. Benzaama, M.-H.; Rajaoarisoa, L.; Boukhelf, F.; El Mendili, Y. Hygrothermal transfer modelling through a bio-based building material: Validation of a switching-linear model. *J. Build. Eng.* **2022**, *55*, 104691. [CrossRef]

81. Švajlenka, J.; Kozlovská, M.; Vranay, F.; Pošiváková, T.; Jámborová, M. Comparison of Laboratory and Computational Models of Selected Thermal-Technical Properties of Constructions Systems Based on Wood. *Energies* **2020**, *13*, 3127. [CrossRef]

82. Caniato, M.; Marzi, A.; Bettarello, F.; Gasparella, A. Designers' expectations of buildings physics performances related to green timber buildings. *Energy Build.* **2022**, *276*, 112525. [CrossRef]

83. Latif, E.; Ciupala, M.A.; Tucker, S.; Wijeyesekera, D.C.; Newport, D.J. Hygrothermal performance of wood-hemp insulation in timber frame wall panels with and without a vapour barrier. *Build. Environ.* **2015**, *92*, 122–134. [CrossRef]

84. Pavelek, M.; Prajer, M.; Trgala, K. Static and dynamic thermal characterization of timber frame/wheat (Triticum Aestivum) chaff thermal insulation panel for sustainable building construction. *Sustainability* **2018**, *10*, 2363. [CrossRef]

85. Bros-Williamson, J.; Garnier, C.; Currie, J.I. A longitudinal building fabric and energy performance analysis of two homes built to different energy principles. *Energy Build.* **2016**, *130*, 578–591. [CrossRef]

86. Latif, E.; Ciupala, M.A.; Wijeyesekera, D.C. The comparative in situ hygrothermal performance of Hemp and Stone Wool insulations in vapour open timber frame wall panels. *Constr. Build. Mater.* **2014**, *73*, 205–213. [CrossRef]

87. Johansson, P.; Hagentoft, C.-E.; Kalagasidis, A.S. Retrofitting of a listed brick and wood building using vacuum insulation panels on the exterior of the facade: Measurements and simulations. *Energy Build.* **2014**, *73*, 92–104. [CrossRef]

88. Fedorczak-Cisak, M.; Radziszewska-Zielina, E.; Orlik-Kożdoń, B.; Steidl, T.; Tatara, T. Analysis of the Thermal Retrofitting Potential of the External Walls of Podhale's Historical Timber Buildings in the Aspect of the Non-Deterioration of Their Technical Condition. *Energies* **2020**, *13*, 4610. [CrossRef]

89. Bishara, N.; Pernigotto, G.; Prada, A.; Baratieri, M.; Gasparella, A. Experimental determination of the building envelope's dynamic thermal characteristics in consideration of hygrothermal modelling—Assessment of methods and sources of uncertainty. *Energy Build.* **2021**, *236*, 110798. [CrossRef]

90. Mahmoodzadeh, M.; Gretka, V.; Hay, K.; Steele, C.; Mukhopadhyaya, P. Determining overall heat transfer coefficient (U-Value) of wood-framed wall assemblies in Canada using external infrared thermography. *Build. Environ.* **2021**, *199*, 107897. [CrossRef]

91. Koh, C.H.; Kraniotis, D. Hygrothermal performance, energy use and embodied emissions in straw bale buildings. *Energy Build.* **2021**, *245*, 111091. [CrossRef]

92. Tlaiji, G.; Ouldboukhitine, S.; Pennec, F.; Biwole, P. Thermal and mechanical behavior of straw-based construction: A review. *Constr. Build. Mater.* **2022**, *316*, 125915. [CrossRef]

93. Koh, C.H.; Kraniotis, D. A review of material properties and performance of straw bale as building material. *Constr. Build. Mater.* **2020**, *259*, 120385. [CrossRef]

94. Sun, K.; Zheng, C.; Wang, X. Thermal performance and thermal transmittance prediction of novel light-gauge steel-framed straw walls. *J. Build. Eng.* **2023**, *67*, 105973. [CrossRef]

95. Miljan, M.; Miljan, J. Thermal Transmittance and the Embodied Energy of Timber Frame Lightweight Walls Insulated with Straw and Reed. *IOP Conf. Ser. Mater. Sci. Eng.* **2015**, *96*, 012076. [CrossRef]

96. Douzane, O.; Promis, G.; Roucoult, J.-M.; Le, A.-D.T.; Langlet, T. Hygrothermal performance of a straw bale building: In situ and laboratory investigations. *J. Build. Eng.* **2016**, *8*, 91–98. [CrossRef]

97. D'Alessandro, F.; Bianchi, F.; Baldinelli, G.; Rotili, A.; Schiavoni, S. Straw bale constructions: Laboratory, in field and numerical assessment of energy and environmental performance. *J. Build. Eng.* **2017**, *11*, 56–68. [CrossRef]

98. Cascone, S.; Catania, F.; Gagliano, A.; Sciuto, G. Energy performance and environmental and economic assessment of the platform frame system with compressed straw. *Energy Build.* **2018**, *166*, 83–92. [CrossRef]

99. Cascone, S.; Evola, G.; Gagliano, A.; Sciuto, G.; Parisi, C.B. Laboratory and in-situ measurements for thermal and acoustic performance of straw bales. *Sustainability* **2019**, *11*, 5592. [CrossRef]

100. Cornaro, C.; Zanella, V.; Robazza, P.; Belloni, E.; Buratti, C. An innovative straw bale wall package for sustainable buildings: Experimental characterization, energy and environmental performance assessment. *Energy Build.* **2020**, *208*, 109636. [CrossRef]

101. Sabapathy, K.A.; Gedupudi, S. In situ thermal characterization of rice straw envelope of an outdoor test room. *J. Build. Eng.* **2021**, *33*, 101416. [CrossRef]

102. Wang, Y.; Huang, J.; Wang, D.; Liu, Y.; Zhao, Z.; Liu, J. Experimental investigation on thermal conductivity of aerogel-incorporated concrete under various hygrothermal environment. *Energy* **2019**, *188*, 115999. [CrossRef]

103. Danovska, M.; Huang, J.; Wang, D.; Liu, Y.; Zhao, Z.; Liu, J. Simulation uncertainty in heat transfer across timber building components in the Italian climates: The role of thermal conductivity. *Energy Build.* **2022**, *268*, 112190. [CrossRef]

104. Jerman, M.; Černý, R. Effect of moisture content on heat and moisture transport and storage properties of thermal insulation materials. *Energy Build.* **2012**, *53*, 39–46. [CrossRef]

105. Wang, Y.; Liu, K.; Liu, Y.; Wang, D.; Liu, J. The impact of temperature and relative humidity dependent thermal conductivity of insulation materials on heat transfer through the building envelope. *J. Build. Eng.* **2022**, *46*, 103700. [CrossRef]

106. Boukhattem, L.; Boumhaout, M.; Hamdi, H.; Benhamou, B.; Nouh, F.A. Moisture content influence on the thermal conductivity of insulating building materials made from date palm fibers mesh. *Constr. Build. Mater.* **2017**, *148*, 811–823. [CrossRef]

107. Rahim, M.; Douzane, O.; Le, A.T.; Langlet, T. Effect of moisture and temperature on thermal properties of three bio-based materials. *Constr. Build. Mater.* **2016**, *111*, 119–127. [CrossRef]

108. Coelho, G.B.A.; Henriques, F.M.A. Influence of driving rain on the hygrothermal behavior of solid brick walls. *J. Build. Eng.* **2016**, *7*, 121–132. [CrossRef]

109. Fernandes, M.S.; Rodrigues, E.; Gaspar, A.R.; Costa, J.J.; Gomes, Á. The impact of thermal transmittance variation on building design in the Mediterranean region. *Appl. Energy* **2019**, *239*, 581–597. [CrossRef]

110. Ihara, T.; Gustavsen, A.; Jelle, B.P. Effect of facade components on energy efficiency in office buildings. *Appl. Energy* **2015**, *158*, 422–432. [CrossRef]

111. Imbabi, M.S.-E. Modular breathing panels for energy efficient, healthy building construction. *Renew. Energy* **2006**, *31*, 729–738. [CrossRef]

112. Leskovar, V.Ž.; Premrov, M. Design Approach for the Optimal Model of an Energy-Efficient Timber Building with Enlarged Glazing Surface on the South Façade. *J. Asian Archit. Build. Eng.* **2012**, *11*, 71–78. [CrossRef]

113. Ge, H.; Baba, F. Dynamic effect of thermal bridges on the energy performance of a low-rise residential building. *Energy Build.* **2015**, *105*, 106–118. [CrossRef]

114. Baba, F.; Ge, H. Dynamic effect of balcony thermal bridges on the energy performance of a high-rise residential building in Canada. *Energy Build.* **2016**, *116*, 78–88. [CrossRef]

115. Ahern, C.; Norton, B.; Enright, B. The statistical relevance and effect of assuming pessimistic default overall thermal transmittance coefficients on dwelling energy performance certification quality in Ireland. *Energy Build.* **2016**, *127*, 268–278. [CrossRef]

116. Ge, H.; Baba, F. Effect of dynamic modeling of thermal bridges on the energy performance of residential buildings with high thermal mass for cold climates. *Sustain. Cities Soc.* **2017**, *34*, 250–263. [CrossRef]

117. Žigart, M.; Kovačič Lukman, R.; Premrov, M.; Žegarac Leskovar, V. Environmental impact assessment of building envelope components for low-rise buildings. *Energy* **2018**, *163*, 501–512. [CrossRef]

118. Košir, M.; Pajek, L.; Iglič, N.; Kunič, R. A theoretical study on a coupled effect of building envelope solar properties and thermal transmittance on the thermal response of an office cell. *Sol. Energy* **2018**, *174*, 669–682. [CrossRef]

119. Fernandes, M.S.; Soares, N.; Gomes, A.; Gaspar, A.R.; Costa, J.J. The potential impact of low thermal transmittance construction on the European design guidelines of residential buildings. *Energy Build.* **2018**, *178*, 379–390.

120. Liu, Z.; Zhou, X.; Tian, W.; Liu, X.; Yan, D. Impacts of uncertainty in building envelope thermal transmittance on heating/cooling demand in the urban context. *Energy Build.* **2022**, *273*, 112363. [CrossRef]

121. *GB 50176-2016*; Code for Thermal Design of Civil Building. China Architecture & Building Press: Beijing, China, 2016.

122. Williamson, A.; Finnegan, S. Sustainability in Heritage Buildings: Can We Improve the Sustainable Development of Existing Buildings under Approved Document L? *Sustainability* **2021**, *13*, 3620. [CrossRef]

123. Papadopoulos, A.M. Forty years of regulations on the thermal performance of the building envelope in Europe: Achievements, perspectives and challenges. *Energy Build.* **2016**, *127*, 942–952. [CrossRef]

124. Yang, X.E.; Liu, S.; Zou, Y.; Ji, W.; Zhang, Q.; Ahmed, A.; Han, X.; Shen, Y.; Zhang, S. Energy-saving potential prediction models for large-scale building: A state-of-the-art review. *Renew. Sustain. Energy Rev.* **2022**, *156*, 111992. [CrossRef]

125. Franceschini, P.B.; Neves, L.O. A critical review on occupant behaviour modelling for building performance simulation of naturally ventilated school buildings and potential changes due to the COVID-19 pandemic. *Energy Build.* **2022**, *258*, 111831. [CrossRef]

126. Chen, Y.; Guo, M.; Chen, Z.; Chen, Z.; Ji, Y. Physical energy and data-driven models in building energy prediction: A review. *Energy Rep.* **2022**, *8*, 2656–2671. [CrossRef]

127. Bienvenido-Huertas, D.; Guo, M.; Chen, Z.; Chen, Z.; Ji, Y. Review of in situ methods for assessing the thermal transmittance of walls. *Renew. Sustain. Energy Rev.* **2019**, *102*, 356–371. [CrossRef]